Journal of Materials Chemistry B

Accepted Manuscript

ROYAL SOCIETY OF CHEMISTRY

www.rsc.org/materialsB

Journal of Materials Chemistry B

ARTICLE

Received 00th January 20xx,

Accepted 00th January 20xx

DOI: 10.1039/x0xx00000x

www.rsc.org/

Multi-Stimuli-Responsive Magnetic Assemblies as Tunable Releasing Carriers

Xiao-Mei Zhang,[a] Kun Guo, [a] Luo-Hao Li ,[b] Sheng Zhang [b*] and Bang-Jing Li [a*]

A novel approach has been developed to prepare the magnetic micelles. Polyethylene glycol (PEG) and poly (N-isopropylacrylamide) (PNIPAM) are firstly attached on the surface of the magnetic nanoparticle via the host-guest inclusion between ferrocene groups (Fc) and β-cyclodextrin (β-CD). Then the resulting MNPs became amphiphilic in water above the LCST of PNIPAM and self-assembled into magnetomicelles with the size of 250 nm. These hybrid micelles show high loading capacity for anticancer drug (DOX) and high saturation magnetization simultaneously. Furthermore, these micelles could disassemble under the effects of oxidant or temperature, providing an opportunity to fine-tune the release properties of encapsulated drug in response to temperature, H_2O_2 or pH independently, or a combined effect of multiple stimuli. Taking other advantages of magnetic carriers, such as high sensitivity to external magnetic field, constrast effect to magnetic resonance, and magnetic hyperthermia, the micelles developed by this study show great potential application in cancer treatment.

Introduction

Magnetic nanoparticles (MNPs) offer exciting opportunities to develop drug delivery systems which simultaneously achieving drug targeting, controlled drug release, and biomedical imaging. The loading drugs in MNPs could be transported to the desired area inside the body by means of an external magnetic field, released at controlled rate in response to environmental stimuli, and tracked using magnetic resonance imaging (MRI) techniques[1].

Normally, the magnetic drug delivery systems were mainly fabricated by two strategies: (1) encapsulated MNPs in an inorganic or a polymeric coating and then conjugated or physical absorbed drug on the surface of particles[2]; (2) encapsulated a mixture of drugs and MNPs in polymeric particles[3]. However, for drug delivery purposes, the drug-storage capacity of the above both structural models are relatively low. And the polymeric drug carriers having better drug loading capacity always suffer significant losses in magnetization[4]. Rattle-type MNPs with a cavity have been developed as efficient drug carriers very recently, which combine the high drug capacity and magnetization. But the preparation of the rattle-type MNPs carriers involves complicated multistep coating, middle layer removal, reduction, and drug loading processes[5,6]. Furthermore, the drug release of most reported rattle-type MNPs follows Fick's diffusion, which cannot be accomplished in a precise control over the location.

In the present work, we develop a novel kind of magnetic micellar aggregates by self-assembly of polymer-grafted magnetic Fe_3O_4 particles. These assemblies embed magnetic Fe_3O_4 as the inner shell and are able to encapsulate large quantities of drugs within the core domain during the self-assembly process, combining the high drug capacity and magnetization simultaneously. The polymer-grafted magnetic particles are prepared by introducing thermally responsive poly (*N*-isopropylacrylamide) (PNIPAM) chain and polyethylene glycol (PEG) chain on the surface of magnetic Fe_3O_4 nanocrystals via redox-switchable inclusion complexation between the β-cyclodextrin (β-CD) and ferrocene (Fc) groups. As a result, the magnetic assemblies show interesting multi-responsive behaviour and are able to tunable release the encapsulated drugs in response to a single stimulus or combinations of stimuli. Scheme 1 illustrates the preparation of magnetic assemblies and their responsive behaviour. In addition, Fe_3O_4 is known to be used not only for magnetically targeted drug delivery, but also magnetic hyperthermia and as a magnetic resonance imaging (MRI) contrast agent. Therefore, the magnetic drug delivery assemblies developed by this study are expected to act as multifunctional platforms for bioimaging and anticancer drug delivery.

Chengdu Institute of Biology, Chinese Academy of Sciences, Chengdu 610041, China, Tel: +86-28-85228831. Fax: (+86)28-85223843. E-mail: libj@cib.ac.cn (B. Li)

State Key Laboratory of Polymer Materials Engineering, Polymer Research Institute of Sichuan University, Sichuan University, Chengdu 610065, China, Tel, Fax: +86-28-85400266. E-mail: zslbj@163.com (S. Zhang)

Electronic Supplementary Information (ESI) available: [details of any supplementary information available should be included here]. See DOI: 10.1039/x0xx00000x

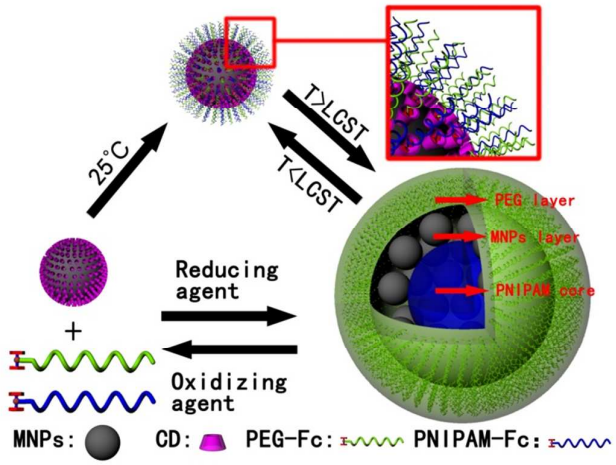

Scheme 1 Illustration of the construction of amphiphilic MNPs by CD inclusion and the thermo-and redox-triggered self-assembly of amphiphilic MNPs.

Results and discussion

Preparation of polymer-grafted MNPs

PEG and thermal-responsive PNIPAM were selected to graft on the MNPs (Fe_3O_4 particles). In order to endow multi-responsive property to MNPs, the attachment of polymer was realized by a redox-responsive β-CD and Fc pair.

Firstly, the Fe_3O_4 magnetic nanoparticles were prepared by the traditional co-precipitation method[7]. β-CD were capped onto the surface of Fe_3O_4 MNPs through the nucleophilic substitution reaction of the Mono-6-(p-tolylsulfonyl)-β-cyclodextrin (6-Ts-β-CD) with MNP-NH_2 moiety. (see the supplementary information for details). The processes were monitored with FT-IR (Fig. S1) and XRD (Fig. S2). Thermogravimetric analysis (TGA) showed that the amount of β-CD on the surface of CD-MNPs was 5.9 wt% (Fig. S3). Assuming the nanoparticles to be spherical[8], the average number of CD units surrounding one MNP was calculated to be 829. TEM and DLS data (Fig. S4) revealed that CD-MNPs showed better water dispersibility than the bared MNPs. Statistics of the TEM results from about 100 CD-MNPs showed a relatively narrow size distribution (30±0.5 nm). As the DLS was carried out in the water dispersion, there is a hydration shell around the particle, the diameter of CD-MNPs obtained by DLS was slight bigger than TEM.

PEG and PNIPAM with Fc as terminal groups were prepared via reaction ferrocene carboxylic acid with PEG and amine-terminated PNIPAM respectively (see supporting information for detailed preparation and characterization).

Studies have showed that CD receptors immobilized onto MNPs maintained their host binding ability toward guest molecules[9]. Mixing the guest polymers and CD-MNPs in the aqueous solution, the polymers were attached on the surface of the CD-MNPs driven by inclusion complexation between β-CD and Fc. FT-IR spectra of CD-MNPs and PEG/PNIPAMCD-MNPs (Fig. S7) showed that the polymer PEG and PNIPAM were grafted on the CD-MNPs and the amount of PNIPAM and PEG attached on the CD-MNPs was 60 wt% as obtained by TGA (Fig. S8)

Assembly and disassembly of PEG/PNIPAM/CD-MNPS

PNIPAM is the most studied thermal-sensitive polymers, which shows sharp transition from a dehydrated to a hydrated state at a temperature below the low critical solution temperature (LCST) of about 32 °C[10]. In our case, the PEG/PNIPAM/CD-MNPs hybrid inclusion complexes (HIC) inherited the thermal-sensitive property of PNIPAM. Below the LCST of PNIPAM, the HIC were stable nanoparticles around 40 nm (Figure 1a), in which both PEG and PNIPAM served as a solvated shell coupled with a magnetic core. As the environmental temperature was elevated above the LCST, PNIPAM turned to hydrophobic while PEG chains kept their hydrophilic property. As a result, the amphiphilic MNPs were formed. Amphiphic block copolymers are well-known to self-assemble into robust nanostructures in aqueous solution[11]. It has been reported that amphiphilic inorganic nanoparticles can be considered as polymer-nanocrystal-polymer analogue of conventional amphiphic polymers and were able to self-assemble into various structures, including micelles and vesicles[12]. Figure 1b showed the transmission electron microscopy (TEM) image morphology of PEG/PNIPAM/CD-MNPs at 37 °C. Larger and narrowly-distributed assemblies around 250 nm were observed. In these assemblies, there was not an obvious contrast between the interior and the shell of the particles, therefore, we regarded the assemblies as micelles[13]. The Fe_3O_4 hydrophobic nanocrystals were expected to locate at the interface between hydrophilic PEG shell and hydrophobic PNIPAM core (as shown in Scheme 1).

The critical micellization concentration (CMC) of amphiphilic PEG/PNIPAM/CD-MNPs in aqueous solution was investigated using pyrene as a fuorescence probe. It was reported that once the micelles form in aqueous solution, the hydrophobic pyrene can be encapsulated into hydrophobic

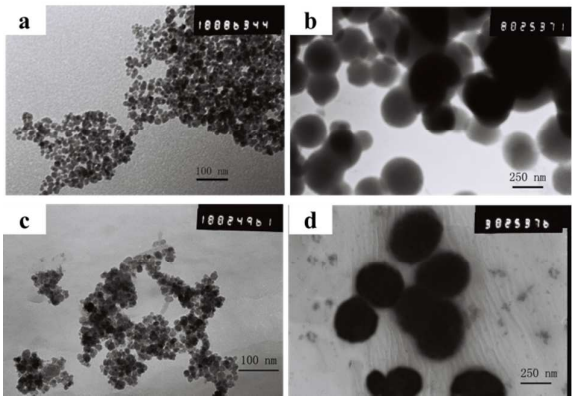

Fig. 1 TEM images of the PEG/PNIPAM/CD-MNP assemblies at 25 °C (a) and 37 °C (b) respectively, and after addition of 5% H_2O_2 (c) or 1% $NaHSO_3$ (d) at 37 °C

microdomains that causes a decrease of the intensity ratio of the first to third band (I_1/I_3) in the pyrene fluorescence emission spectrum[14]. Fig. 2 showed that the I_1/I_3 ratio started to decrease and reached a constant value with the increase of PEG/PNIPAM/CD-MNPs concentration at 37 °C. From the plot of pyrene I_1/I_3 ratio, the CMC of the amphiphilic PEG/PNIPAM/CD-MNPs was estimated to be 0.01 mg/mL.

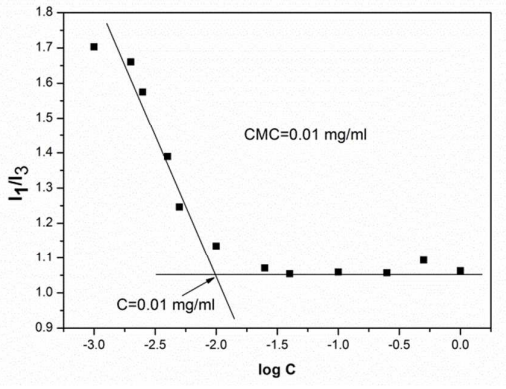

Fig.2 Influence of amphiphilic MNPs concentration on the I_1/I_3 ratio of pyrene fluorescence at 37 °C

Several heating-cooling processes were performed between 25 and 37 °C, the dynamic light scattering (DLS) data demonstrated that the transition between single PEG/PNIPAM/CD-MNPs particles and large micelles was completely reversible and reproducible (Fig. S9).

Inclusion complexation between β-CD and Fc is well-known reversible controlled by the redox state of Fc[15]. Fc in its reduced state, as a neutral compound, binds strongly to CDs, while in its oxidized state ferrocenium (Fc^+), as a cation, binds very weakly. Therefore, the association/dissociation of PEG/PNIPAM/CD-MANPs could be triggered by redox reaction. As shown in the Fig. 1c, the micelles disassembled into dispersed particles (40 nm) after the addition of oxidizing agents H_2O_2, while the assemblies formed again (around 250 nm) when reducing agents 1% $NaHSO_3$ was added, as the Fig. 1d presented. In the presence/absence of H_2O_2, the PEG/PNIPAM/CD-MNPs solution was centrifuged at 37 °C at 14,000 rpm. TGA data indicated that the micellar aggregates were composed of polymer and CD-MNPs simultaneously in the absence of H_2O_2 (Figure S10a). However, in the presence of H_2O_2, the particles only consisted of CD-MNPs (Figure S10b). These results suggested that the PEG/PNIPAM/CD-MNPs micelles dissociated into CD-MNPs after the addition of oxidant due to the decomplexation of β-CD and Fc.

Encapsulation of DOX within PEG/PNIPAM/CD-MNPS micelles.

The multi-sensitive PEG/PNIPAM/CD-MNPs micelles are good candidates for the controlled drug delivery. Here, doxorubicin (DOX), a first-line chemotherapeutic agent, was selected as a model molecule to investigate their capability as a carrier system. The DOX were encapsulated in PEG/PNIPAM/CD-MNPs micelles by a solvent-evaporation method. According to the UV-vis absorption spectra (Fig. S11), the DOX encapsulation efficiency was calculated to be 73%, and the DOX loading capacity was 170 μg of drug/mg of micelles. This drug loading capacity was far more than that of polymeric magnetic micelles or vesicles[16] and even more than the core-shell hollow magnetic mesoporous silica particles[5a].

The room temperature magnetization curves of PEG/PNIPAM/CD-MNPs micelles were shown in Fig. 3a. It can be seen that the specific saturation magnetization (Ms) of DOX-loaded magnetic micelles was 33.10 emu g^{-1}, which was smaller than for pure Fe_3O_4 (69.20 emu g^{-1}). The decrease in the value of Ms could be attributed to the coated polymer and DOX loading. In comparison with the magnetic drug delivery system formed in other way[17], the value of Ms is quite high, ensuring that these magnetic micelles can be efficient manipulated under a low strength magnetic strength. As shown in Fig. 3b, the suspended PEG/PNIPAM/CD-MNPs micelles were easily collected using a magnet within 30s. The hysteresis loops have negligible coercivity (Hc), indicating the superparamagnetism of PEG/PNIPAM/CD-MNPs micelles. This superparamagnetism property meant that capillary block by aggregation formed by residual magnetism after removal of external field will be avoided.

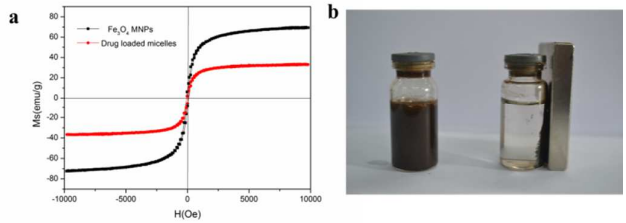

Fig. 3 (a): Magnetization curves of DOX-loading micelles and Fe_3O_4-MNPs, (b): A macroscopic view of drug-loaded micelles in an external magnetic field.

The tunable release of DOX

The diverse responsiveness to external stimuli of PEG/PNIPAM/CD-MNPs micelles provides an opportunity to fine-tune the release properties of drug.

The thermally triggered release of DOX was investigated by entrapped micelles in a dialysis bag and measured DOX concentration in external PBS solutions at different time intervals. As shown in Fig. 4a, the release of DOX at 25 °C was much quickly than that at 37 °C. Within 720 min, 28% of DOX were released at 25 °C, while only 10% DOX were released at 37 °C. This thermally sensitive release behaviour was induced by the disassembly of the micelles. At 37 °C, PEG/PNIPAM/CD-MNPs formed micelles, which encapsulated DOX in the hydrophobic PNIPAM core. The DOX were released by slowly diffusion. At 25 °C, the PNIPAM shifted from hydrophobic to hydrophilic, causing the magnetic micelles to disassemble into stable small CD-MNPs covered by PEG and PNIPAM, thus triggering a burst of DOX release in the first 100 min. It should be noticed that this thermal-induced release was incomplete (more than half of the DOX remained even after 800 min), which possibly because the interactions between uncharged DOX and PNIPAM chains kept some DOX on surface of single small PEG/PNIPAM/CD-MNPs particles.

Similar results also have been shown in PEG-PNIPAM vesicles[18]. Therefore, the DOX-loaded magnetic micelles could first release free DOX and MNPs/DOX at the site of a tumor when coupled to hypothermic patches and local cryosurgery probes, then the MNPs/DOX can be taken up by tumour cells, acting as miniature munitions.

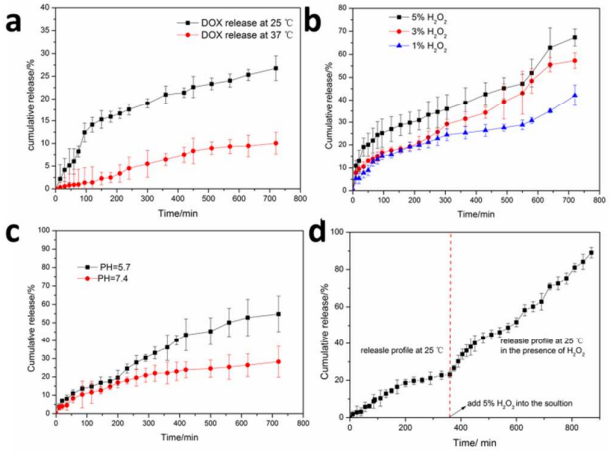

Fig. 4 The cumulative release of DOX from the magnetic micelles triggered by (a) temperature (b) H_2O_2 and (c) pH or (d) temperature and H_2O_2 dual stimuli

Due to the redox-triggered association/dissociation behaviour of PEG/PNIPAM/CD-MNPs, the DOX could also be released at controlled rate by the addition of H_2O_2. As shown in Fig. 4b, a large amount of DOX was released in response to H_2O_2. With the increase of concentrations of H_2O_2, the release of DOX became faster. As previously discussed, the addition of oxidant caused PEG/PNIPAM/CD-MNPs particles dissociated to CD-MNPs. As a result, encapsulated DOX were released. Since the decomplexation of the β-CD/Fc resulted in the dissociation of PNIPAM chains from CD-MNPs, the DOX absorbed on PNIPAM were able to be detected too, causing the redox-triggered release efficiency of DOX was much higher than thermal-triggered release efficiency. The mechanism of DOX released from PEG/PNIPAM/CD-MNPs micelles triggered by temperature or redox-regent was presented in Scheme 2. Studies have shown that cancer cells produce high amounts of H_2O_2 and high levels of H_2O_2 in cancer cells is essential for cancer development[19], therefore, the H_2O_2-sensitive drug delivery systems are expected to not only release anticancer drug locally in cancer cells, but also decrease the cellular levels to reverse malignant phenotype of cancer cells.

Moreover, the release of DOX from the PEG/PNIPAM/CD-MNPs micelles under different pH values (pH=5.7 and 7.4) was investigated at 25 °C, and the results are shown in Fig. 4c. In the initial 7 h, about 30 % of the DOX was released from the micelles at pH 5.7 (the endosomal pH of a cancer cell), and the release rate at pH 7.4 was almost the same. However, the release efficiency increased faster at pH 5.7 than at pH 7.4 with the time increasing. That may be related to the protonation of NH_2 on the DOX under the acidic condition, similar phenomenon was also observed by other DOX-loaded particles or micelles[20]. These acid-sensitive is also desirable for cancer treatment.

Combining the stimuli, we can get more complex release. Figure 4d shows the two-step release behaviour of DOX. In the first step, DOX release was triggered by temperature. The hybrid micelles dissociated to PEG/PNIPAM/CD-MNPs in the absence of H_2O_2 at 25 °C, causing partial release of DOX. Approximately 23.1% of the DOX was released, and large amount of DOX was still absorbed on PNIPAM chains. The second step of the release was controlled by a combination of temperature and oxidant. When adding H_2O_2 into the system after the thermal-induced release, the PEG/PNIPAM/CD-MNPs particles dissociated to CD-MNPs due to the decomplexation of the β-CD/Fc. As a result, DOX absorbed on the PNIPAM chains was released. After an additional 360 min, the total release of the DOX in response to both stimuli was 89%.

The diverse responsiveness to external stimuli of PEG/PNIPAM/CD-MNPs micelles provides an opportunity to fine-tune the release properties of encapsulated drug to each stimulus independently or to a combined effect of multiple stimuli. The loaded drug can be released locally in the acidic environment and higher H_2O_2 area, where is typical the location of cancer cells.

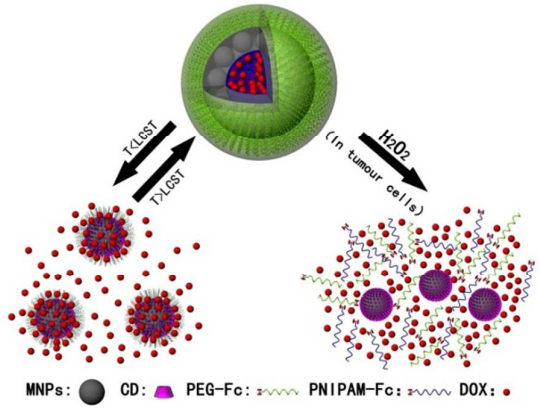

Scheme 2 Illustration of a possible mechanism of DOX released from the PEG/PNIPAM/CD-MNPs micelles triggered by temperature or redox-regent.

Cytotoxicity study

The in vitro cytotoxicity of DOX loaded micelles and free DOX were evaluated on A549 cells. As in shown in Fig. 5, the DOX-loaded micelles displayed a concentration-dependent cytotoxic effect, which was higher than that observed with equivalent doses of DOX in solution. When the DOX-equivalent concentration was 2.5 μg/mL, the cell viabilities for A549 cells of free DOX and DOX-loaded micelles were 61.6% and 65.2% respectively, indicating almost the same activity of DOX in both formulations. However, DOX loaded in the magnetic micelles can be released in the local tumour sites and kill cancer cells in a smart way, which is not achieved by free DOX.

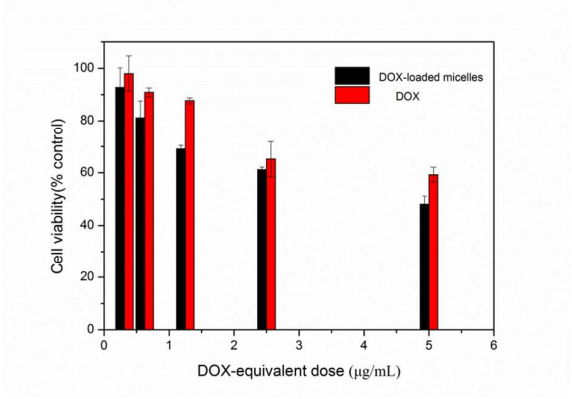

Fig. 5 A549 cell viability after 72 h incubation with different concentration of free DOX and DOX-loaded micelles. Values represent the average± s.d. (n = 5)

Experimental

Materials and methods

Methoxy polyethylene glycol (mPEG, Mn=2000) and poly(N-isopropyl acrylamide), amine terminated (PNIPAM, Mn=2500) were purchased from Sigma-Aldrich (Shanghai China). Ferric chloride hexahydrate ($FeCl_3 \cdot 6H_2O$), 4-(dimethylamino) pyridine (DMAP), dicyclohexylcarbodiimide (DCC), ferrocene carboxylic acid (FcA), 6-chloro-1-hydroxibenzotriazol (HOBT) were purchased from Aladdin Reagent Co., Ltd (Shanghai, China). 6-Ts-β-cyclodextrin was directly used from the work group. All other reagents were of analytical grade and were used directly without further purification. All solvents and water were re-distilled freshly.

Preparation of PEG/PNIPAM modified magnetic nanoparticles and self-assembly micelles.

5 mg CD-MNPs was dispersed in 10 mL deionized water to give the CD-MNPs aqueous solution (0.5 mg · ml^{-1}), 3.8 mg Fc-terminated PNIPAM (1.4×10^{-3} mmol) was first added to the above solution; after stirring for 24 h, 1 mg Fc-terminated PEG (4.7×10^{-4} mmol) was added subsequently (molar ratio of PNIPAM/PEG = 3:1) and stirred for another 24 h. Then, the mixed solution was loaded into a dialysis bag (MWCO 8000-14000) and dialyzed against deionized water for three days to remove the free polymer which was not immobilized onto the surface of the MNPs. When the temperature was adjusted above the low critical solution temperature (LCST) of Fc-terminated PNIPAM, the magnetic nanoparticles became amphiphilic, and the micelles self-assembled from such amphiphilic magnetic nanoparticles could be obtained as a result of the solubility reversal of PNIPAM.

Encapsulation of DOX within PEG/PNIPAM/CD-MNPS micelles

1 mg of PEG/PNIPAM coated MNPs was dispersed in 5 mL deionized water to give an aqueous dispersion of mangnetic micelles. Doxorubicin hydrochloride was first converted to water insoluble base (DOX) using the procedure described previously. An ethanolic solution of DOX (150 μL, 2 mg/mL) was added drop-wise while stirring to the above aqueous dispersion and stirred at 37 °C overnight. The DOX-loaded micelles were collected by centrifugation at 14000 rpm. The mass of DOX in supernatant was determined by UV-vis spectrometry at 485 nm and calculated with the standard curve plotted by the absorbance at 485 nm versus the DOX concentration. The DOX encapsulation efficiency and loading efficiency were calculated using the following equation.

Encapsulation efficiency (%) = (DOX in feed-free DOX) × $(\text{DOX in feed})^{-1}\times100$

Loading capacity= mass of drug loaded in the micelles/ mass of micelles

In vitro release of DOX from the micelles

The release of DOX from the micelles was carried out using the dialysis method. The Dox-loaded micelles were injected into a dialysis bag (MWCO 3500), and dialyzed against the PBS solution at 37 °C to ensure complete removal of any free DOX outside the vesicles.

After the initial aliquot was taken, the dialysis bag was immersed in a 400 ml PBS solution (pH=7.4, I= 0.01 M), DOX were released for 720 min at 37 °C and 25 °C. At predetermined time interval, samples (3 mL) were taken out from buffer solution outside the dialysis bag and replaced with an equal volume of fresh buffer solution. All the release processes were carried out in triplicate. The amount of DOX released was analyzed by fluorescence emission at a λmax of 590 nm, with excitation at 485 nm.

The DOX release profile from DOX-loaded micelles dispersed in 5% H_2O_2, 3% H_2O_2, 1% H_2O_2 were immersed in a 400 ml PBS solution (pH=7.4, I= 0.01 M) at 37 °C. The DOX release profile were investigated under the same conditions as described above.

The release profile of DOX from DOX-loaded micelles under different pH values were investigated at 25 °C and carried out as follows: the dialysis bag filled with DOX-loaded micelles solution was immersed in a 400 ml PBS solution (pH=5.7 and 7.4, I= 0.01 M) at 25 °C and released for 720 min. The amount of DOX released was analysed under the same conditions as described above.

In addition, the DOX release profile under the temperature and oxidant dual stimuli was carried out as follows: the dialysis bag filled with micelles solution was immersed in a 400 mL PBS solution (pH=7.4, I= 0.01 M) at 25 °C for 360 min. Then H_2O_2 was added into the micelles solution and released for another 360 min.

In vitro cytotoxicity of the micelles

Cell viability against the micelles and the drug loaded micelles were measured by MTT assay. A549 cells were seeded in 96-well plates (1×10^5 cells mL^{-1}, 150 μL per well) and incubated with RPMI 1640 medium containing 10 v% fetal bovine serum at 37 °C under a humidified atmosphere with CO_2 (5%) for 24 h. The cells were treated with100 μL per well of fresh media containing with free DOX and DOX-loaded

micelles at varying concentrations of 0.31–5μg DOX-equivalent dose of DOX. After 72 h of incubation, the cell media were replaced by 25 μL of 5μg/mL MTT, and the cells were incubated for another 4h, then the medium was removed, and 150 μL DMSO was added into each well. After 30 minutes, the absorbance of dissolved formazan was measured using a Bio-Rad microplate reader at 570 nm. The cell viability was obtained by calculation according to the ratio of the intensity of purple formazan in viable cells treated in magnetic micelles and DOX loaded micelles to the intensity in untreated control cells.

Conclusions

In summary, we have developed a novel class of magnetic micelles assemblied from PEG and PNIPAM coating magnetic nanoparticles. These PEG/PNIPAM/CD-MNPs micelles show high loading capacity for anticancer drug (DOX) and high saturation magnetization simultaneously. It is demonstrated that the PEG/PNIPAM/CD-MNPs micelles could disassemble under the effects of oxidant or temperature via 1) discomplexation of β-CD-Fc triggered by redox-regent; 2) hydrophobic-to-hydrophilic transition of PNIPAM caused by temperature. This diverse responsiveness to external stimuli of PEG/PNIPAM/CD-MNPs micelles provides an opportunity to fine-tune the release properties of encapsulated drug to temperature, H_2O_2 or pH independently, or to a combined effect of multiple stimuli. The high saturation magnetization ensures that these micelles act a very efficient protocol to targeted drug delivery assisted by magnetic fields. In addition, these hybrid micelles also show great potential in other therapeutic treatments, such as MRI contrast agents, and hyperthermia treatment.

Acknowledgements

This work was funded by the National Natural Science Foundation of China (Grant Nos. 51373174, 21074138, 51073107), the CAS Knowledge Innovation Program (Grant No.KSCX2-EW-J-22) and the Opening Project of State Key Laboratory of Polymer Materials Engineering (Sichuan University).

Notes and references

1 Y. Zhang, W. Ma, D. Li, M. Yu, J. Guo, C. C. Wang, *Small,* 2014, **10**, 1379-1386; X. Mou, Z. Ali, S. Li and N.Y. He, *J. Nanosci. Nanotechnol.*, 2015, **15**, 54-62; H. Oliveira, E. Perez-Andres, J. Thevenot, *J. Control. Release*, 2013, **169**, 165-170.

2 M. M. Yallapu, S. P. Foy, T. K. Jain, V. Labhasetwar, *Pharm. Res.*, 2010, **27**, 2283-2295; T. K. Jain, M. A. Morales, S. K. Sahoo, D. L. Leslie-Pelecky, V. Labhasetwar, *Mol. Pharm.*, 2005, **2**, 194-205.

3 J. Kim, J. E. Lee, T. G. Park, T. Hyeon, *Adv. Mater.*, 2008, **20**, 478-483; H. Ai, C. Flask, B. Weinberg, X. T. Shuai, M. D. Pagel, D. Farrell, J. Duerk, J. M. Gao, *Adv. Mater.*, 2005, **17**,1949-1952.

4 M. Talelli, C. J. F. Rijcken, T. Lammers, P. R. Seevinck, G. Storm, C. F. van Nostrum, W. E. Hennink, *Langmuir*, 2009, **25**, 2060-2067.

5 H. X. Wu, S. J. Zhang, J. M. Zhang, G. Liu, J. L. Shi, L. X. Zhang, X. Z. Cui, M. L. Ruan, Q. J. He, W. B. Bu, *Adv. Funct. Mater.*, 2011, **21**, 1850-1862; F. H. Chen, L. M. Zhang, Q. T. Chen, Y. Zhang, Z. J. Zhang, *Chem. Commun.*, 2010, **46**, 8633-8635; F. Dilnawaz, A. Singh, C. Mohanty, *Biomaterials*, 2010, **31**, 3694-706; X. Li, H. Li, G. Liu, Z. Deng, *Biomaterials*, 2012, **33**, 3013-3024.

7 X. Q. Liu, Z. Y. Ma, J. M. Xing, *J. Magn. Magn. Mater.*, 2004, **270**, 1-6.

8 H. Wang, Y. Chen, X. Y. Li and Y. Liu, *Mol. Pharma.*, 2007, **4**, 189-198.

9 Y. Wu, F. Zuo, Z. Zheng, X. Ding, Y. Peng, Nanoscale. *Res. Lett.*, 2009, **4**, 738-747; K. Hayashi, K. Ono, H. Suzuki, M. Sawada, M. Moriya, W. Sakamoto and T. Yogo, *ACS Appl. Mater. Interfaces.*, 2010, **2**, 1903-1911.

10 P. Kujawa, V. Aseyev, H. Tenhu, *Macromolecules*, 2006, **39**, 7686-7693.

11 G. C. Yu, Y. J. Ma, C. Y. Han, Y. Yao, G. P. Tang, Z. W. Mao, C. Y. Gao, and F. H. Huang, *J. Am. Chem. Soc.*, 2013, **135**, 10310-10313; X. F. Ji , S. Y. Dong , P. F. Wei , D. Y. Xia , and F. H. Huang , *Adv. Mater.,* 2013, **25**, 5725-5729; X. D. Chi , X. F. Ji, D. Y. Xia, and F. H. Huang, *J. Am. Chem. Soc.,* 2015, **137**, 1440-1443.

12 M. S. Nikolic, C. Olsson, A. Salcher, A. Kornowski, A. Rank, R. Schubert, A. Fromsdorf, H. Weller, and S. Forster, *Angew. Chem. Int. Ed.*, 2009, **48**, 2752-2754; J. M. Hu, T. Wu, G. Y. Zhang, S. Y. Liu, *J. Am. Chem. Sci.*, 2012, **134**, 7624-7627; K. C. Wei, J. Li, J. H. Liu, G. S. Chen, M. J, *soft matter*, 2012, **8**, 3300-3303.

13 Z. H. Nie, D.Fava, E. Kumacheva, S. Zou, G. C. Walker and M. Rubinstein, *Nat. Mater.,* 2007, **6**, 609-614; M. S. Nikolic, C. Olsson, A. Salcher, A. Kornowski, A. Rank, R. Schubert, A. Fromsdorf, H. Weller and S. F¨orster, *Angew. Chem. Int. Edit.*, 2009, **48**, 2752-2754.

14 Z. J. Liu, P. Yao, *Polym. Chem.*, 2014, **5**, 1071-1081.

15 M. Nakahata, Y. Takashima, H. Yamaguchi and A. Harada, *Nat. Commun.*, 2011, **2**, 511-518; P. Du, J. Liu, G. Chen, M. Jiang, *Langmuir*, 2011, **27**, 9602-9608; M. Xue, Y.Yang, X. D. Chi, X. Z. Yan, and F. H. Huang, *Chem. Rev.,* 2015, **115**, DOI: 10.1021/cr5005869; G. C. Yu, K. C. Jie , and F. H. Huang, *Chem. Rev.,* 2015, **115**, DOI: 10.1021/cr5005315; X. Z. Yan, F. Wang, B. Zheng and F. H. Huang, *Chem. Soc. Rev.,* 2012, **41**, 6042-6065.

16 T. K. Jain, J. Richey, M. Strand, D. L. Leslie-Pelecky, C. A. Flask, V, *Biomaterials*, 2008, **29**, 4012-4021; N. Nasongkla, E. Bey, J. M. Ren, H. Ai, C. Khemtong, J. S. Guthi, S. F. Chin, A. D. Sherry, D. A. Boothman, and J. M. Gao, *Nano Lett.,* 2006, **6**, 2427-2430; C. Sanson, O. Diou, J. Thevenot, E.Ibarboure, A. Soum, A. Brulet, S. Miraux, E.Thiaudiere, S. Tan, A. Brisson, V. Dupuis, O. Sandre, and S. Lecommandoux. *ACS Nano*, 2011, **5**, 1122-1140.

17 Y. T. Zhang, W. F. Ma, D. Li, *small*, 2014, **10**, 1379-1386; T. B. Ren, Q. M. Liu, H. Lu, *J. Mater. Chem.*, 2012, **22**, 12329-12338.
18 S. Qin, Y. Geng, D. E. Discher and S. Yang, *Adv.Mater.,* 2006, **18**, 2905-2909.
19 M. Lo´pez-La´zaro. *Cancer Lett.*, 2007, **252**, 1-8.
20 X. X. Hu, X. H. Hao, Y. Wu, J. H. Zhang, X. N. Zhang, P. C. Wang, G. Z. Zou, X. J. Liang, *J. Mater. Chem. B*, 2013, **1**, 1109-1118.

Graphical Abstract:

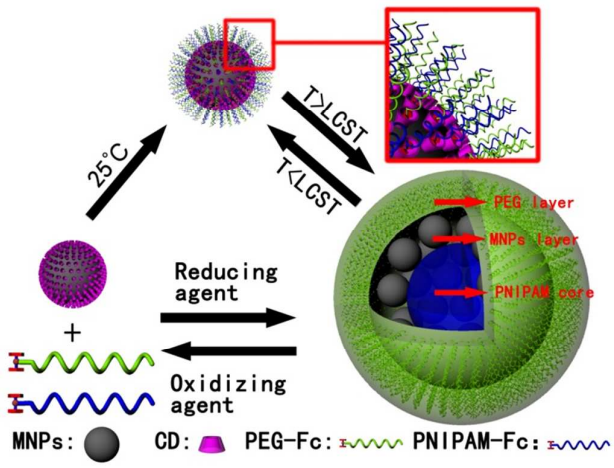

Construction of amphiphilic magnetic nanoparticles (MNPs) by cycledextrin-based inclusion complexation and the reversible assembly of these MNPs triggered by temperature or redox.